Geometric Accuracy of PhaseOne PAS Pana

Karsten Jacobsen [1], Richard Ladstaedter [2], Robert Bosch [3]

[1] Institute of Photogrammetry and GeoInformation, Leibniz Universität Hannover, Germany - jacobsen@ipi.uni-hannover.de
[2] Joanneum Research Digital, Dept. for Remote Sensing and Geoinformation, Graz, Austria – Richard.ladstaedter@joanneum.at
[3] PhaseOne A/S, Frederiksberg, Denmark – rob@phaseone.com

Keywords: Digital Camera, PhaseOne PAS Pana, Configuration, Geometry, Self-Calibration.

Abstract

Due to the currently limited size of CMOS-sensors and the demand for larger capacity imaging systems, camera systems are being used instead of single cameras. Beside smaller systems, PhaseOne produces now the PAS Pana system with a combination of 5 RGB cameras and 2 near infrared (NIR) cameras, each with 14204 x 10652 pixels (Figures 1, 2 and 3). This system captures fused images at 48800 x 12400 pixels in RGB NIR (red line in Figure 1). With the pixel size of 3.76 µm, a fused image has a size of 183.5 mm ∗ 46.6 mm. Through thermal control, the geometry of each individual sub-camera can be almost completely guaranteed. However, this is not possible for such a large camera system, requiring a stitching of the sub-images by adjustment. The overlapping two infrared camera images cover the whole range of the 5 RGB sub-cameras. For this reason, the joint NIR images are used as reference for fusing the RGB sub-cameras. The geometric quality of the fused images is analysed with a block adjustment and it corresponds to the image accuracy of the sub-cameras.

1. Introduction

The PAS Pana camera system (Figures 1 – 3) with 5 red, green and blue (RGB) and 2 near infrared (NIR) sub-cameras, each with 14204 x 10652 pixels, covers a large area. It is possible to use the 7 original images, but the demand is more for a unique RGB and NIR image, which reduces the effort of handling the images.

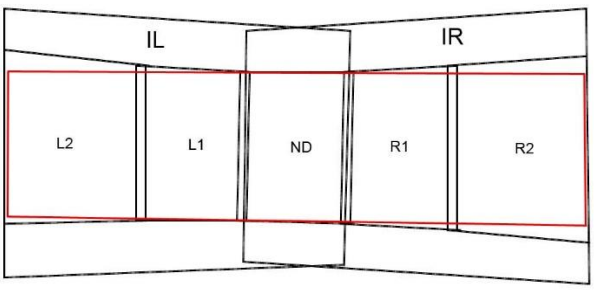

Figure 1. Covered ground area by PAS Pana sub-cameras, IL, IR = infrared cameras +/-14° nadir angle, f=70.01mm RGB-cameras at nadir, +/-13° and +/-27° nadir angles, f=146mm.

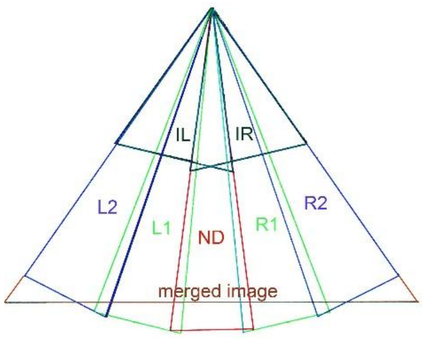

Figure 2. Combination of PAS Pana fields of view.

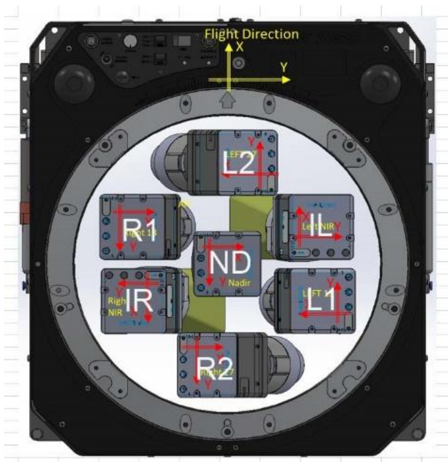

Figure 3. Physical configuration of PAS Pana camera system with the rotation of the sub-cameras.

It is possible to fuse the sub-images with respect to the nadir sub-image (ND) by starting with the first right sub-image (R1) and the first left sub-image (L1), then fusing the second right sub-image (R2) and the second left sub-image (L2) with the previously fused images, and then fitting the both NIR sub-images (IR) and (IL) to the fused RGB images. The overlap of the RGB sub-cameras is limited and carries the risk of failure in case of poor contrast areas. In addition, the error propagation from ND to the other sub-images is not optimal. It would be based on the outer part of the sub-images, which are often influenced by larger systematic errors in the image corners. Initial test were not successful, so fusing the individual RGB images to the joint NIR images was preferred. The NIR images overlap by 30%, which ensures a better connection as the RGB sub-images to the neighboured sub-images.

2. Method

A first test with suboptimal fusing software showed a small change in the relative orientation of neighbouring sub-images (Figure 4) over a sequence of 197 images, thus confirming the experiences of the authors from other camera systems. Even under optimal conditions, a tie of the RGB-images is difficult due to the small overlap. Due to suboptimal results, the fusing procedure is in development by JOANNEUM RESEARCH, Institute for Digital Technologies by fusing the RGB-images to the joint near infrared images.

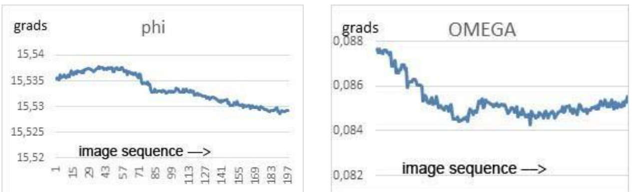

Figure 4. Change of phi and omega over 197 near infrared images.

The Brown-Conradi parameters (identical to Australis) (2) and (3) were used as standard additional parameters for camera calibration. These parameters cannot detect and take into account systematic image errors, which are different for the individual image corners. The problems started with the rotation of the Brown-Conradi parameters. The calibration was performed with the large format side in the horizontal direction. Rotation of the Brown-Conradi parameters is possible, but for the parameters P1, P2 and B1 and B2 only with a slight change in the exterior orientation, which affects the direct sensor orientation. Of course, these effects are small and not so important, but should not be neglected. Finally, more difficult are the geometric effects at the image corners, which can reach up to 3 µm. These effects can be extrapolated to the entire image, which should be avoided. With the complete parameter set of BLUH program system, these corner effects can be determined and taken into account. If a correction grid is used for the images instead of the values of the additional parameters, the problem of the rotation influence to the self-calibration does not exist.

The near-infrared images have a larger overlap and can connect the RGB-images better. For this reason, the fusion of all 7 sub-images was performed at all tie points between the RGB-images and the stitched near-infrared images. This fusion also eliminates the largest part of the previously mentioned small problems.
However, in areas with water surfaces, it may not be possible to stitch the 7 images together. However, as we can see in Figure 4, the changes in the orientation of overlapping near-infrared images are small and not sudden changes, but correspond to a slow drift of the parameters. That is, areas with fusion problems can be bridged by interpolating orientations of neighboured images in the flight lines. This procedure was used by (Dörstel et al 2002) also for the DMC-I camera, which is based on 4 sub-cameras, and resulted in sub-pixel accuracy.

Due to the lack of time, an error occurred in the processed Denver dataset, so when fusing the sub-camera images into a homogenous joint image, the JOANNEUM RESEARCH got the results of a flight calibration instead of the laboratory calibration of the sub-cameras. The flight calibration data are not identical to the laboratory calibration, and more importantly, the flight calibration is not rotated as shown in Figure 3. In addition to the not correctly rotated Brown-parameters B1, B2, P1 and P2, the not negligible location of the principle point was also not handled correctly. It was not possible to repeat the merging with the correct calibration data and the correct rotation up to the deadline of the Istanbul workshop. However, as already mentioned, large parts of the geometric problems are compensated by stitching the sub-images. The projection centres of the seven sub-cameras have an offset from each other and from the centrally located nadir camera. The influence of the offset on the image coordinates is small, especially at higher flight altitudes, and could be taken into account. In fact, this is nearly compensated by fusing the images.

3. Used Denver Data Set

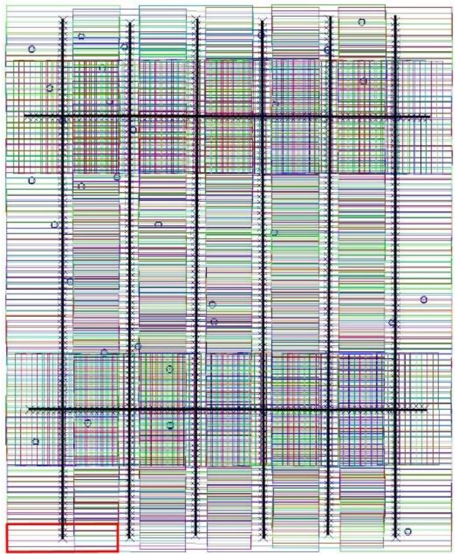

Figure 5. Covered area, flight lines, location of GCP.
Lower left = highlighted single image.

The Denver photo flight was conducted from an altitude of ~6000m above ground, resulting in a ground resolution of 17cm for the fused images. The North-South flight strips have 40 % side overlap and 75 % end overlap. Two crossing flight lines cover 44% of the entire area (Figure 5). There are 36 ground control points (GCP) in the area. In the 718 images, 193818 ground points and 1.2 million image points were determined, resulting in an average of 6.5 images / object point.

4. Self-calibration

Even a perfect camera calibration will be affected by inevitable geometric changes of a camera system. Of course, some of this will be compensated by the fusion mentioned above, but not all of it. As usual, a self-calibration can improve the accuracy of a block adjustment.

Systematic image errors can be determined and taken into account by bundle block adjustment with self-calibration using additional parameters, but the set of additional parameters used must be able to fit to the geometric problems of the images used. Remaining systematic image errors after self-calibration with additional parameters can be analysed using residuals at the image coordinates after bundle adjustment. By superimposing all image residuals in one image plane the residuals can be averaged into small image sub areas (Jacobsen et al. 2010). Based on the remaining systematic image errors determined in this way, the set of additional parameters can be extended to cover these effects. This method also has the advantage, that it avoids strong correlations between the parameters.

Systematic image errors can be determined and described by additional parameters (1) up to (4) during self-calibration. A more flexible and easier to handle description of the systematic image errors by using the formulas is the use of an image correction grid based on self-calibration, as is available for the BLUH program. If additional parameters need to be added for a specific image geometry, the programs using the correction grid do not need to be changed.

Additional parameters of Brown-Conradi (Australis)

$x = x_{meas} - xp \quad y = y_{meas} - yp$ (1) inner orientation
x, y = image coordinates
xp, yp = principal point
$r^2 = x^2 + y^2$
$dr = K1 * r^3 + K2 * r^5 + K3 * r7$ (2) radial symmetric
K1, K2, K3 radial symmetric distortion parameters
$x_{corr} = x_{meas} – xp – x*dr/r + P1*(r^2+2*x^2)+2*P2*x*y + B1 * x + B2*y$
$y_{corr} = y_{meas} .yp + y*dr/r + P2*(r^2 + 2*y^2) + 2*P1*x*y$ (3)
P1, P2 decentering distortion parameters
B1, B2 affinity and angular affinity (non-orthogonal)
(2) + (3) = Brown-Conradi (Australis) self-calibration parameters (User Manual for Australis, 2007)

Additional parameters of BLUH

Overview (4)
1 = angular affinity, 2 = affinity
3 - 6 = general distortion
7 - 8 = tangential distortion
9 = r^3 (~K1) but with zero crossing
10 - 11 radial symmetric higher degree F(sin(r))
12 = general distortion
13 = focal length 14, 15 = principal point
26 – 33 = original Australis (Brown-Conradi) parameters
81 – 88 radial and tangential distortion of corners
90 - 97 as 81 – 88, but limited to 1/3 of range from corner
160 – 194 special parameters for PAS Pana

x, y = image coordinates normalized to maximal radial distance 162.6mm (scale factor: 162.6 / maximal radial distance)
$r^2 = x^2 + y^2 \quad b = \arctan(y/x)$

1. x' = x - y•P1 y' = y - x•P1
2. x' = x - x•P2 y' = y + y•P2
3. x' = x - x•cos 2b • P3 y' = y - y•cos 2b • P3
4. x' = x - x•sin 2b • P4 y' = y - y•sin 2b • P4
5. x' = x - x•cos b • P5 y' = y - y•cos b • P5
6. x' = x - x•sinb • P6 y' = y - y•sin b • P6
7. x' = x + y•r•cos b • P7 y' = y - x•r•cos b • P7
8. x' = x + y•r•sin b • P8 y' = y - x•r•sin b • P8
9. x' = x - x•(r^2-16384) •P9 y' = y - y•(r^2 - 16384) •P9
10. x ' = x - x•sin(r • 0.049087) • P10 y' = y - y•sin(r • 0.049087) • P10
11. x' = x - x•sin(r • 0.098174) • P11 y' = y - y*sin(r •0.098174) • P11
12. x' = x - x•sin 4b • P12 y' = y - y• sin 4b •P12
14. x' = x – px principle point x
15. y' = y - py principle point y

81.$x' = x + x*x*y*y*ABS(x*y)*10^{-9}$
$y' = y - x*x*y*y*ABS(x*y)*10^{-9}$
radial only for upper left corner x<0. y>0. limit
82.$x' = x + x*x*y*y*ABS(x*y)*10^{-9}$
$y' = y + x*x*y*y*ABS(x*y)*10^{-9}$
tangential only for upper left corner x<0. y>0. limit
83 – 88 corresponding for other corners
90 – 97 similar, but only for 1/3 of limit

160 up to 190 special parameters for PAS Pana

160 – 163 shift x separately for R1, R2, L1, L2
164 – 167 shift y separately for R1, R2, L1, L2
168 – 172 rotation for ND, R1, R2, L1, L2
173 - 177 curvature $\Delta x* (y*y)$ for ND, R1, R2, L1, L2
$x' = x + \Delta x*y* y*Pn$ Δx from right sub-image limit
178 – 182 curvature $-\Delta x * (y*y)$ for ND, R1, R2, L1, L2
$x' = x - \Delta x*y* y*Pn$ Δx from left sub-image limit
183 - 186 affinity for R1, R2, L1, L2
187 - 190 angular affinity for R1, R2, L1, L2
191 – 194 shift and affinity for L2

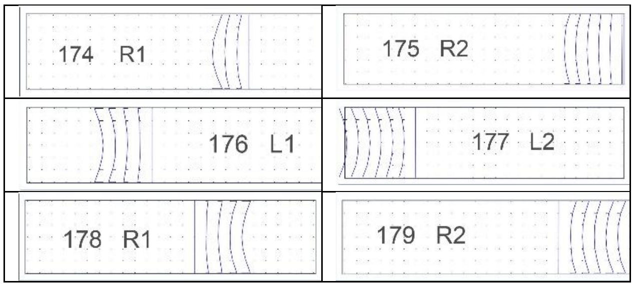

Figure 6. Influence of special PAS Pana additional parameters separated for the sub-area of the sub-cameras.

The additional parameters used in BLUH are formulated in such a way that there is a low correlation between the additional parameters and to the inner orientation. This can be analyzed using the total correlation, which expresses how the influence of one parameter can be replaced by the group of all other. The correlation is reduced by the used parameters, for example, the affinity parameter (parameter 2) is positive for x and negative to y, avoiding a correlation to the focal length. This is not the case for the Brown-Conradi parameters, where the affinity parameter B1 only depends on x, causing a correlation with the focal length. Similarly, the radial symmetric distortion is used in BLUH with a zero crossing, reducing the correlation with the focal length, while this is not the case with the Brown-Conradi parameters. The radial symmetric Brown-Conradi parameters K1, K2 and K3 are strongly correlated to each other with a correlation coefficient between r=0.98 and r=0.92 and correlate to the focal length with r=0.58 up to 0.69.

Systematic image errors can be determined and described using self-calibration by additional parameters (3) up to (5). A more flexible and easier to handle description of the systematic image errors as by use of the formulas is the use of an image correction grid based on self-calibration, as is available for the BLUH program. If for a specific image geometry additional parameters need to be added the programs using the correction grid do not need to be changed.

By bundle block adjustment with self-calibration by additional parameters, systematic image errors can be determined and respected, but the set of additional parameters used must be able to fit to the geometric problems of used images. Remaining systematic image errors after self-calibration with additional parameters can be analysed through residuals at the image coordinates after bundle adjustment and this can be used for new additional parameter which should be added to the existing set.

5. Results of Bundle Block Adjustment

For the bundle block adjustment with the BLUH program the special PAS Pana parameters 160 up to 194 (4) have been included into BLUH corresponding to possible and determined geometric problems. The block adjustments are just based on ground control points. Direct sensor orientation was not used due to the influence of the incorrect use of the inner orientation on the location of the projection center. Figure 5 shows that block adjustment using direct sensor orientation is not necessary for this block configuration.

5.1 Without Self-Calibration

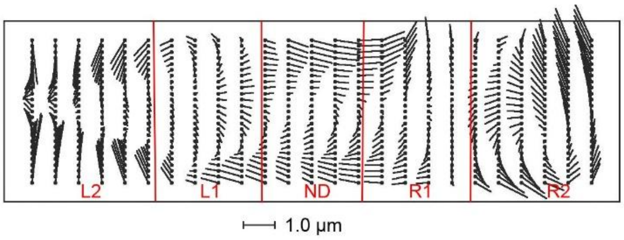

Figure 7. Remaining systematic image errors of adjustment without self-calibration with the range of the sub-images in red.

The remaining systematic image errors of the block adjustment without self-calibration (Figure 7) have just a root mean square of 0.47 µm up to 0.55 µm. The root mean square of the image coordinates (in BLUH identical to sigma 0) with 1.13 µm (0.3 ground sampling distance (GSD)) is small. This inconspicuous size should not be misinterpreted. The remaining systematic image errors are just showing a part of the real size. However, Figure 7 shows, that the sub-images fit well. There are no sudden changes in the remaining systematics from one sub-image to the adjacent one, indicating that the fusion of the sub-images and the reference near infrared images was performed with satisfactory accuracy.

5.2 Adjustment with Brown-Conradi Parameters

The total correlation (Table 1) describes how the additional parameter can be replaced by all others together. As typical, the radial symmetric parameters K1 up to K3 are strongly correlated. All parameters are significant at the 99.9% level. The Student test, which is identical to the relationship of the size of the additional parameter divided by its standard deviation, is large for the decentering parameters P1 and P2.

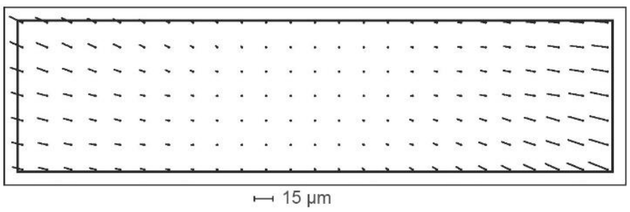

Figure 8. Systematic image errors based on Brown-Conradi additional parameters.

The systematic image errors based on the Brown-Conradi parameters (Figure 8) are dominated by the decentering distortion parameters P1 and P2 (3).

TOTAL CORRELATION	0.964	0.992	0.978	0.015	0.001	0.016	0.001
ADDITIONAL PARAMETERS	26	27	28	30	31	32	33
	K1	K2	K3	B1	B2	P1	P2
STUDENT TEST	25.97	47.39	42.32	14.46	12.13	80.14	120.27

Table 1. Statistical information of Brown-Conradi parameters.

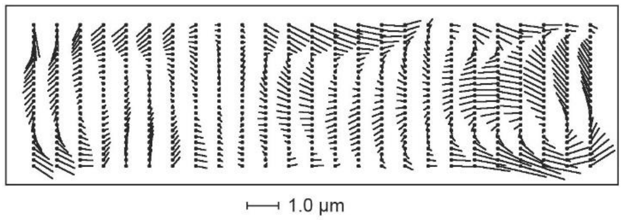

Figure 9. Remaining systematic image errors based on the Brown-Conradi parameters.

The remaining systematic image errors have a root mean square value of 0.37 µm. The shape (Figures 7 and 9) cannot be eliminated using the Brown-Conradi parameters.

5.3 Adjustment with BLUH Parameters

5.3.1 Basic Parameters + Principal Point (1-12, 14-15): The standard BLUH additional parameters result in systematic image errors corresponding to a curvature of the fused PAS Pana images (Figure 10) (left side up, right side up), that is different as for the Brown-Conradi parameters (Figure 7). However, the remaining systematic image errors (Figure 11) are similar to the remaining systematic image errors of Brown-Conradi (Figure 9).

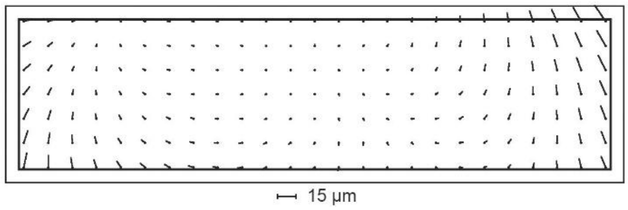

Figure 10. Systematic image errors based on BLUH parameters 1-12 and 14-15 (basic+ principal point x and y).

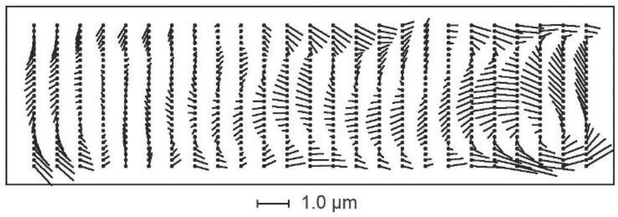

Figure 11. Remaining systematic image errors based on the BLUH parameters 1-12 and 14-15.

5.3.2 Standard Parameters + Principal Point + Corner (1-12, 14-15 + 81-88):

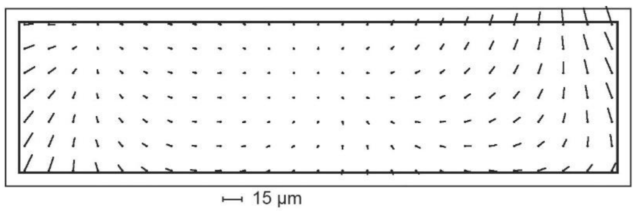

Figure 12. Systematic image errors based on BLUH parameters 1-12 and 14-15 + 81-88 (Corner parameter).

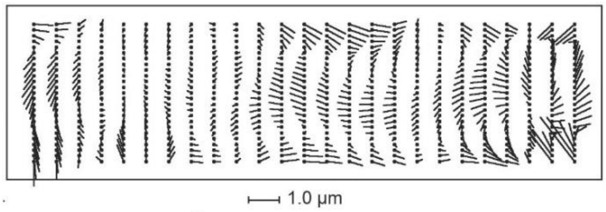

Figure 13. Remaining systematic image errors based on the BLUH parameters 1-12, 14-15, 81-86 (corner parameter).

The corner parameters 81-88 only improve the corners of the systematic image errors (Figure 12) and the corners of the remaining systematic image errors, but do not change the general trend of the remaining systematic image errors.

5.3.3 Standard Parameters + Principal Point + Corner + Special PAS Pana Parameter (1-12, 14-15 + 81-88 + 130-194): The complex shape of the remaining systematic image errors without the special PAS Pana parameter (Figures 6, 9, 11 and 12) requires a larger set of additional parameters, separately for the image areas of the sub-cameras. Parameters 160 up to 172 are shifts in x and y and a rotation. Parameters 183 up to 190 stand for affinity and angular affinity. The parameters 173 up to 182 are special parameters for the curvature in y-direction linear depending on the x-coordinate. These parameters were specifically developed according to the shape of the remaining systematic image errors. Figure 15 shows that the remaining systematic image errors can be largely reduced. With this set of additional parameters, the sigma0 is reduced to 0.94 µm and the remaining systematic image errors to 0.16 µm.

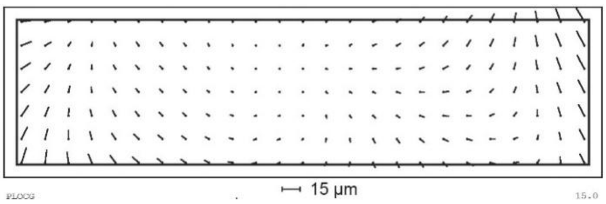

Figure 14. Remaining systematic image errors based on the BLUH parameters 1-12 and 14-15 + 81-88 + 160-194. Systematic image errors based on BLUH parameters 1-12 and 14-15 + 81-88 + 160-194.

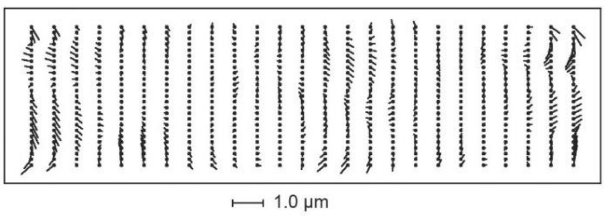

Figure 15. Remaining systematic image errors based on the BLUH parameters 1-12, 14-15, 81-86 and the special PAS Pana parameters 160 – 194

ADDITIONAL PARAMETERS

1	1000	2000	3000	4000	5000	6000	7000	8000	9000	10000	11000	12000
2	14000	15000	81000	82000	83000	84000	85000	86000	87000	88000	160000	161000
3	162000	163000	164000	165000	166000	167000	168000	169000	170000	171000	172000	173000
4	174000	175000	176000	177000	178000	179000	180000	181000	182000	183000	184000	185000
5	186000	187000	188000	189000	190000	191000	192000	193000	194000			

STUDENT TEST

1	164.80	48.61	111.44	101.40	90.04	17.95	241.68	158.87	195.05	16.80	2.66	124.10
	+++	+++	+++	+++	+++	+++	+++	+++	+++	+++	++	+++
2	18.25	9.06	16.14	13.82	30.78	50.34	28.28	4.18	22.54	37.85	5.17	13.48
	+++	+++	+++	+++	+++	+++	+++	+++	+++	+++	+++	+++
3	46.36	30.56	82.39	88.84	94.57	31.62	17.61	63.17	54.81	96.69	36.64	2.21
	+++	+++	+++	+++	+++	+++	+++	+++	+++	+++	+++	+
4	5.44	7.76	1.52	1.54	4.98	5.06	10.62	0.83	4.08	8.77	25.69	13.49
	+++	+++			+++	+++	+++		+++	+++	+++	+++
5	17.58	33.68	49.21	80.16	35.38	34.65	14.56	43.29	43.70			
	+++	+++	+++	+++	+++	+++	+++	+++	+++			

Table 2. Student test of the additional parameters as Figure 15.

5.4 Dependency on the Image Numbers

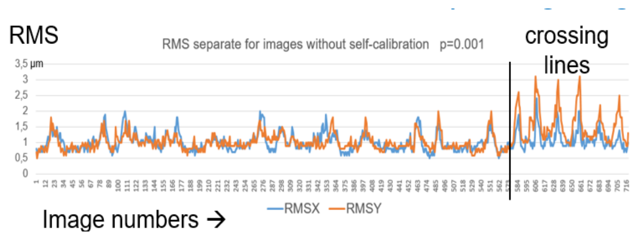

Figure 16. Root mean square image coordinate discrepancies of block adjustment without self-calibration depending on the image numbers.

The root mean square coordinate discrepancies of the block adjustment without self-calibration, sorted by the image numbers (Figure 16), show a clear influence caused by the named problem of the pre-calibration for the images of the crossing flight lines. With strong image tie, the systematic errors cannot be compensated by the image orientation.

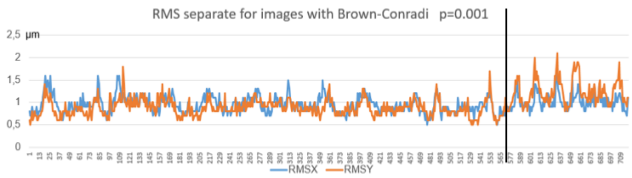

Figure 17. Root mean square image coordinate discrepancies of block adjustment with Brown-Conradi parameters depending on the image numbers.

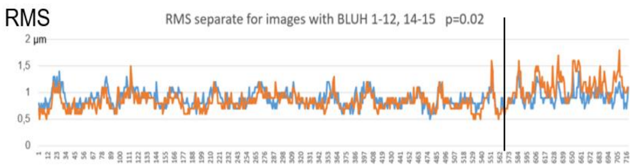

Figure 18. Root mean square image coordinate discrepancies of block adjustment with basic BLUH parameters depending on the image numbers.

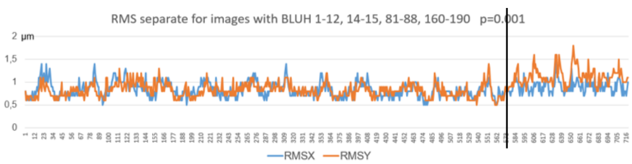

Figure 19. Root mean square image coordinate discrepancies of block adjustment with basic and the special PAS Pana parameter of BLUH depending on the image numbers.

Additional parameter →	without	Brown-Conradi	basic BLUH	Pana set BLUH
Minimal X	0.50	0.53	0.48	0.46
Minimal Y	0.54	0.50	0.50	0.48
Maximal X	2.37	1.79	1.86	1.49
Maximal Y	2.52	1.86	1.87	1.50
RMS X	1.06	0.98	0.94	0.86
RMS Y	1.18	0.98	0.96	0.90

Table 3. Results of individual image root mean square [µm] after block adjustment with different sets of additional parameter.

In particular, the block adjustment without self-calibration shows some problems with the images with the crossing flight lines, which caused by the problems of the camera pre-calibration (Figures 16-19), with root mean square differences of the individual images of up to 2.5 microns (Table 3). This is of course not very large, but can be reduced to a maximum of 1.5 microns and in the root mean to 0.9 microns (Table 3) by the special PAS Pana additional parameters of BLUH. The systematic image errors in the crossing flight lines cannot be partially compensated by the image orientation, as is the case for the north-south flight lines.

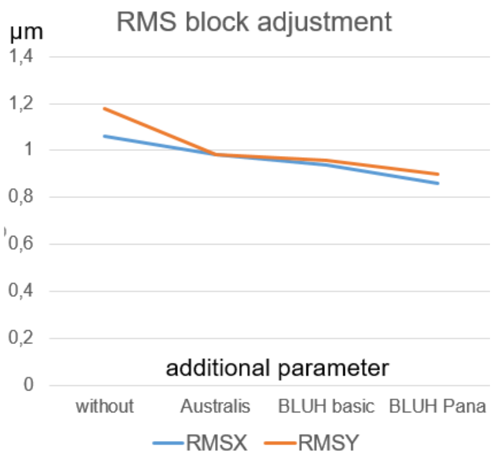

Figure 20. Root mean square image coordinates as function of self-calibration. 1: Without, 2: Australis 3: basic BLUH, 4: BLUH PAS Pana parameter.

The rot mean square of the image coordinates is significantly reduced by the self-calibration. The standard set of additional parameters through the Brown-Conradi (Australis) parameters and the standard BLUH-parameters improves the result, but as shown before, the special PAS Pana parameters are required.

6. Conclusion

Of the 57 additional parameters used in chapter 5.3.3, only 3 are not significant (Table 2). If they are the automatically or manually excluded from the adjustment, the result does not change. The bundle block adjustment was computed with an a priori standard deviation of the ground control points of 0.02 m, corresponding to the accuracy of the GCP ground survey, and with 0.01 m, and 0.001 m. With the small a priori standard deviation, the block stronger can be fitted to the GCP. The systematic image errors and the remaining systematic image errors are only slightly changed by the weight of the GCP.

The images of the PAS Pana sub-cameras used in for the Denver flight campaign were fused by the JOANNEUM RESEARCH to homogenous images. Due to time pressure, the JOANNEUM RESEARCH got not the correct calibration data including a wrong kappa rotation of the calibration data. This resulted in a systematic deformation of the fused images. Systematic deformation can be determined by self-calibration with additional parameters, but the used parameters must be able to compensate the deformation. Even due to the operational problems, the achieved root mean square image coordinates (sigma0) in the range of 1.0 µm or 0.26 pixels are at the level what is reached with digital cameras with just one CMOS sensor. At the limit of the sub-cameras' sub-areas, no geometric problems can are evident in the fused PAS Pana images (see the plots of the remaining systematic image errors above).

Tables 4 to 6 show the limited influence of the GCP weight on sigma0 and the root mean square of the remaining systematic image errors. The root mean square of the ground control points is strongly influenced by the weight, especially for the Z-component. The advantage of the special PAS Pana additional parameters is very clearly visible in the Z-component. The disadvantage of the Brown-Conradi parameters is obvious. However, it must be taken into account that the direct sensor orientation was not used due to the problems in handling the sub-camera calibration. Using the direct sensor orientation as observation in the bundle block adjustment, would reduce the influence of the systematic image errors on the object coordinates. The accuracy reached (Table 6, last line) corresponds in X and Y to 0.6 respectively 0.5 GSD. The vertical accuracy of 24 cm corresponds to 1.4 GSD, which is very good for the base to height relation in direction of flight of approximately 1:4 or a standard deviation of the x-parallax of 0.35 GSD.

	RMS X	RMS Y	**RMS Z**	Sigma 0	RMS remaining
Without self-calibration	0.38m	0.35m	**1.74m**	1.13µm	0.47µm
Brown-Conradi parameters	0.35m	0.22m	**1.67m**	1.03µm	0.37µm
Add par 1-12, 14-15	0.34m	0.21m	**1.07m**	1.01µm	0.35µm
Add par 1-12, 14-15, 81-86	0.36m	0.22m	**0.79m**	0.99µm	0.33µm
Add par as above + 160-190	0.39m	0.24m	**0.44m**	0.94µm	0.16µm

Table 4. Results of block adjustments with a priori SX,SY,SZ=0.02, RMSX, RMSY, RMSZ at GCP, RMS remaining at image coordinates after adjustment.

	RMS X	RMS Y	**RMS Z**	Sigma 0	RMS remaining
Without self-calibration	0.32m	0.29m	**1.30m**	1.13µm	0.48µm
Brown-Conradi parameters	0.28m	0.17m	**1.19m**	1.04µm	0.38µm
Add par 1-12, 14-15	0.27m	0.16m	**0.83m**	1.01µm	0.36µm
Add par 1-12, 14-15, 81-86	0.28m	0.17m	**0.60m**	1.00µm	0.33µm
Add par as above + 160-190	0.30m	0.18m	**0.37m**	0.94µm	0.16µm

Table 5. Results of block adjustments with a priori SX, SY, SZ=0.01.

	RMS X	RMS Y	**RMS Z**	Sigma 0	RMS remaining
Without self-calibration	0.13m	0.12m	**0.49m**	1.20µm	0.55µm
Brown-Conradi parameters	0.10m	0.08m	**0.42m**	1.07µm	0.41µm
Add par 1-12, 14-15	0.09m	0.08m	**0.39m**	1.05µm	0.34µm
Add par 1-12, 14-15, 81-86	0.10m	0.08m	**0.32m**	1.02µm	0.34µm
Add par as above + 160-190	0.10m	0.08m	**0.24m**	0.97µm	0.15µm

Table 6. Results of block adjustments with a priori SX, SY, SZ=0.001m.

The Brown-Conradi parameter set (identical to Australis) is often used for standard camera calibration. This parameter set can be used to determine the radial symmetric image errors, but for other geometric effects only the decentering distortion P1 and P2 as well as the affinity and angular affinity parameters B1 and B2 are available. The BLUH program includes a larger set of additional parameters, including also special corner parameters. For the handling of the fused PAS Pana images an additional special set of parameters was developed. With BLUH the remaining systematic errors have been reduced to 0.16 µm in the root mean square, causing also a reduction of the root mean square Z-differences at the ground control points by 75%. This was not possible with the Brown-Conradi additional parameters. So also with the not correct calibration information for the PAS Pana sub-cameras satisfying results of the block adjustment was reached with a sigma0 of 0.94 µm. In BLUH sigma0 is identical to the standard deviation of the image coordinates.

This result confirms the quality of fusing the PAS Pana sub-images by the method in development by JOANNEUM RESEARCH. In addition, the developed set of special additional parameters has the flexibility to compensate even not correct camera calibration information. An improvement of the fusion is possible by use of a correction grid. This correction grid can be rotated without problems and has no influence to the exterior orientation, as it is the case with the Brown-Conradi parameters.

Acknowledgement

We would like to thank Phase One and the US company Surdex for the support of the investigation.

References

Doerstel, C., Zeitler, W., Jacobsen, K., 2002. Geometric Calibration of the DMC: Method and Results. *IntArchPhRS*, (34) Part 1 Com I, 324-333.

Jacobsen, K., Cramer, M., Ladstaedter, R., Ressl, C., Spreckels, V., 2010. DGPF project: Evaluation of digital photogrammetric camera systems - geometric performance. PFG, *2010(2)*, 85–98.

User Manual for Australis, 2007. Photometric Photogrammetry Software, photometrix.com.au, Accessed October 2024.